Reconfigurable Compact Quad-port MIMO Antennas for sub-6 GHz Applications

Qasim Hadi Kareem[1,a)], Rana Ahmed Shihab[2)]

[1]Computer Engineering Department, Al-Farabi University College, Baghdad, Iraq.
[2]QA & Accreditation office, Al-Farabi University College, Baghdad, Iraq.

Corresponding E-mail:qasim.hadi2017@gmail.com[a)]

Abstract
This paper presents compact quad-port frequency reconfigurable multi-input multi-output (MIMO) antennas for 5 G applications that operate at sub-6 GHz. The proposed design provides more isolation (>13 dB) and pattern diversity using four orthogonal radiating elements. C-shaped metal is used to extend the antenna's radiating elements by inserting one positive intrinsic negative diode (PIN) in the metal. The C-shaped metal and matching stub achieve frequency reconfigurability with a consistent radiation pattern. The PIN diode's switching characteristics allow the frequency to be shifted between two communication bands. One mode (diode ON) covers 2.5 and 5 GHz, while the second mode (diode OFF) covers another dual band of 3.5 and 5.7 GHz. Substrate dimensions are only 50 x 50 x1.6 mm3, making the proposed design compact. Antenna peaks at a gain of 4.18 dB and radiation efficiencies of 80 and 94% in the four frequency bands. The antenna design is appropriate for multi-functional wireless systems and cognitive radio applications since it spans frequency bands below 6 GHz and can be reconfigurable between wide and narrow bands.

Keywords: MIMO antennas, sub-6 GHz, Reconfigurable Antenna, stubs, Cognitive radio

1. INTRODUCTION

Because of the development of mobile devices, security cameras, and multi-band gadgets, cognitive radio (CR) is now used by Internet of Things (IoT) devices. Numerous wireless communication applications, such as automated home/office and smart classrooms, utilize this CR's several frequency bands. Other applications include biotelemetry and intelligent vehicle networks. Short-range communication between dissimilar devices can be accomplished via various frequency bands, including narrow and wideband. When employing several radio frequency bands, it is necessary to have a small device with antennas. In recent decades, researchers have found a solution to this challenge by designing reconfigurable antennas that can simultaneously operate in wide and narrowband modes. However, increasing these devices' data rate and throughput is also a challenge [1, 3].

The MIMO idea fixes this issue by keeping RF specifications intact. As a result, frequency reconfigurable wideband-to-narrowband MIMO antennas appear to be a possible solution to the abovementioned issue.

One of the most important technologies for 5G communication is MIMO, which allows

systems to achieve peak data speeds and improved spectrum efficiency [4, 8]. As a result, it significantly increases throughput capacity over standard SISO systems. Compared to SISO, MIMO offers better gain, bandwidth, channel capacity, and diversity performance. Using MIMO technology, higher data rates can be achieved without sacrificing airwaves or transmitted power [9, 10].

The critical challenges during the design process for MIMO antenna systems for mobile devices are related to the antenna sections' needs for low coupling and compactness. Although the potential capacity of a MIMO antenna system increases due to coupling the signals received at different antenna elements [11], this does not improve the system's actual capacity. In addition, the system cannot provide the diversity advantage when the envelope correlation coefficient (ρ) is greater than 0.5, as stated in [12].

In recent years, antennas for 5G communications that work in the sub-6 GHz range have been reported in [13, 26] for different reconfigurable MIMO devices and fixed dual-band elements. For example, a paper [13] shows that a quad-antenna, concentric pentagonal based slot-line reconfigurable MIMO system can be tuned from 1.32 to 1.49 GHz and 1.75 to 5.2 GHz. [14] presents a frequency-reconfigurable MIMO antenna based on an annular slot design. As reported in [15], a wide and continuous frequency band antenna system is described. An ultrawideband (UWB) sensing antenna with a four-element reconfigurable MIMO antenna is demonstrated. From 0.75 GHz up to 7.65 GHz, the UWB sensing antenna can pick up signals. The 2.32–2.45 GHz, 2.52–2.75 GHz, and 3.4–3.6 GHz (m-WiMAX) bands can be reconfigured using a frequency reconfigurable MIMO antenna system [16]. In this system, the DC bias of the PIN diodes on each slot line controls isolation. For example, the suggested antenna spans the frequency range between 1.8 and 2.45 gigahertz. 5G (3.5 GHz) systems with several antennas have been described in [17, 19]. A twelve-port MIMO antennas array for

multi-band operation (LTE bands 42, 3.4–3.6 GHz, 43, 3.6–3.8 GHz, and 46, 5.1–5.9 GHz) is built of three antenna parts [20]. In [21] a dual-band MIMO antenna had been described. This antenna includes two modules, one for 4G (2 x 2 MIMO configuration) and one for 5G (8 x 8 MIMO configuration). The use of two orthogonally positioned PIFA pairs in a dual-band MIMO antenna for LTE and WiMAX mobile applications has been proposed in [22]. Antenna modules support the LTE band (40/42), 5G bands, and Wi-Fi bands, making the antennas complex and bulky. In the 5G application sub-6 GHz band, a small dual band with an inherent filtering structure has been presented in [23]. According to reports, these new antennas do not allow user customization regarding frequency band selection. Two-port dual-band MIMO antennas capable of tuning/reconfiguring their operational frequencies between 2.5 and 3.6 GHz have been described [24]. An RF switch with a single pole and four throws is utilized to fine-tune the frequency. Furthermore, using a differential-fed antenna allows it possible to enable switchable WLAN applications in addition to sub-6 GHz 5G ones [25]. In switching the frequency spectrum, PIN diodes that can be controlled electronically are used. According to [26], metal-rimmed frequency reconfigurable antennas can be used in smartphones. Two separate types of antenna modules, operating in two distinct frequency bands (4G and 5G), are employed in this system. Module 1 operates in the low-band (0.82–0.96 GHz), the intermediate band (1.71–2.17 GHz), and the high-band (2.30–2.69 GHz) using a varactor diode, whereas module 2 operates in the fixed 5 G spectrum. It has also been found that only a small number of MIMO systems antenna circuits can reconfigure their frequencies.

In this paper, MIMO antennas can support 4G and 5G technologies in LTE band 40 (2300–2400 MHz), LTE band 41 (2490–2690 MHz) and sub-6 GHz LTE band 42 (3400–3600 GHz), LTE band 43 (3600–3800 MHz) using a basic quasi-planar structure. A single PIN diode can switch two distinct frequency

ranges (state-1 and state-2 for 4G and 5G bands, respectively). Four quasi-planar antennas are integrated and placed orthogonally on the same substrate using a self-isolation technique for the designed MIMO antennas. Because of its high isolation (>13 dB) and low envelope correlation coefficient, the MIMO system's gain diversity is validated by this configuration. The simulated antenna properties, including the reflection coefficient, surface current distribution, gain, ECC, radiation patterns, and efficiency are assessed and discussed in this article.
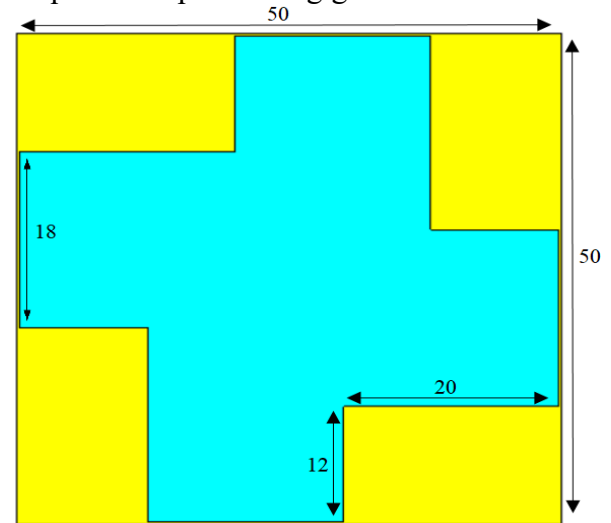
The following is a summary of the most significant contributions made by the work that was presented:

(i) The size of the antenna is smaller than in previous work in this field, and in addition to this, it offers multi-band mode, enhanced bandwidth, and gain.

(ii) According to the authors' available information, this research accomplishes an unprecedented frequency selectivity across four bands while delivering the most significant number of beam directions possible.

(iii) An antenna with pattern and frequency reconfigurability is particularly well suited to 5G services
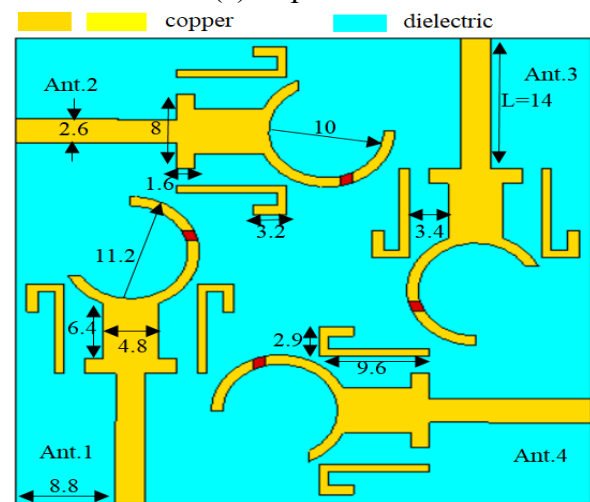
2. ANTENNAS CONFIGURATION

Figure 1 shows the proposed antenna's configuration. The images depict the top and bottom views, respectively. The substrate is made of 1.6-millimeter thick FR4 material for the antenna, with a relative permittivity of 4.4 and an overall area of 50 x 50 mm2, with the antenna printed on it. The ground plane on the FR4 substrate's bottom side is the antenna ground. Four identical patch antenna elements referred to as Ant1 - Ant4, are proposed for placement orthogonally around the substrate's four edges. The patch antenna has a surface area of 33 x 11.2 mm2. 50 Ohm microstrip lines are used to feed each component. PIN diodes are used to create a reconfigurable section of a circle to tune the frequency. Low-distortion toggles can benefit from using a PIN diode (SMP1345-040LF) to avoid high

RF voltages. This diode operates most well at frequencies up to three gigahertz.
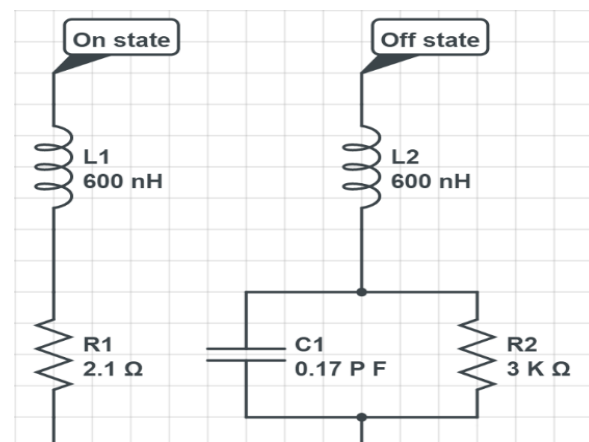

(a) Top view.

(b) Bottom view

Figure 1. Layout of the reconfigurable MIMO antennas.

Figure. 2. Equivalent circuit of PIN diode.

Figure 2 represents the equivalent PIN diode circuit utilized in this device's development.

The OFF state of the PIN diode was modeled as a parallel configuration with a resistance of 3K Ω and capacitance of 0.17pF. The ON state of the PIN diode was represented as a 2.1 Ω resistor. Switching the diode enabled a continuous dual-frequency reconfigurable band.

2.1 Single Antenna
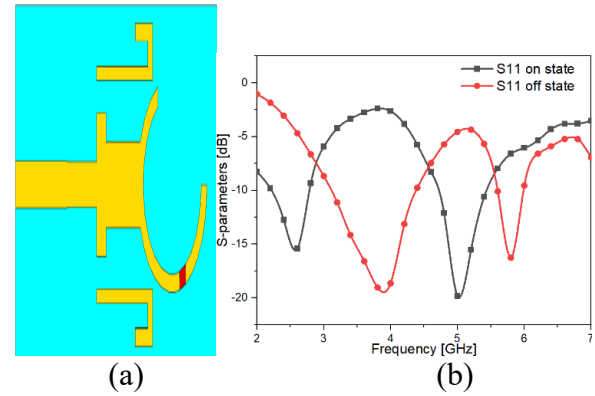
One of the four-port elements is shown schematically in Figure 3. A rectangular patch antenna element with a compact area of 33 x 11.2 mm2 on the substrate board is a good starting point. A low return loss at the required frequency can only be achieved with good impedance matching between the patch antenna and the transmission line by moving the 50 Ohm microstrip feedline, as illustrated. CST Microwave Studio, an electromagnetic solver, is used to model the proposed antenna. A lack of bandwidth and compactness make patch antennas ineffective in today's wireless systems. However, these concerns can be overcome with appropriate modifications.

Figure 3b depicts the reflection coefficients for the ON and OFF states. Two steps can be included in the patch element to increase the bandwidth for operating bands.

Figure 1 shows the specifics of each parametric dimension of the design, which were derived following a thorough parametric analysis. The following relationship [27] aims to estimate the radiator's length (L) parameter to perform a specific frequency operation in equation (1) and (2):

$$L = \frac{c}{4f\sqrt{\varepsilon_{eff}}}$$ 　　　　Eq.1

$$\varepsilon_{eff} = \frac{\varepsilon_r+1}{2} + \frac{\varepsilon_r-1}{2}\left(1 + 12\left(\frac{w}{h}\right)\right)^{-0.5}$$ 　Eq.2
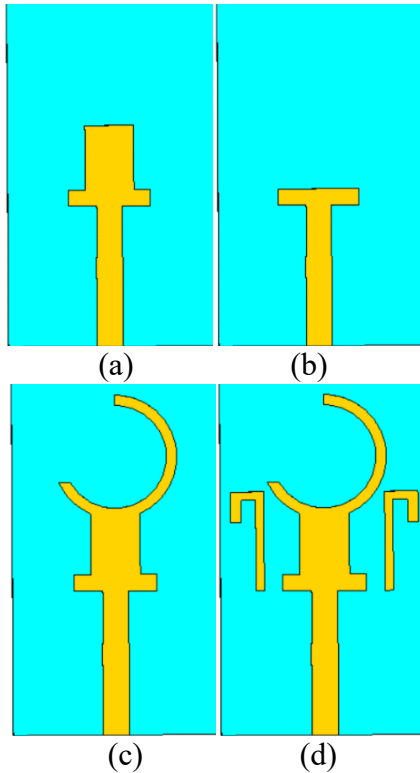
Where h denote the thickness, c the speed light in a vacuum, and w is the width of the substrate.
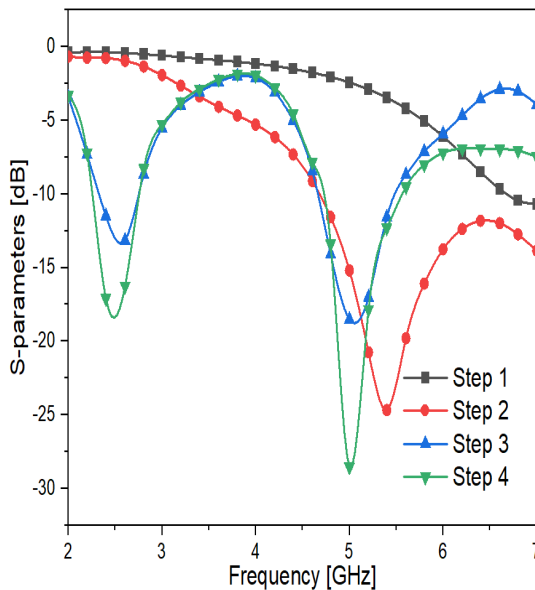

(a)　　　　　　　　　　(b)

Figure 3. Schematic of single antenna and its reflection coefficients (a) Single antenna (b) Reflection coefficients

A pin diode switch (SMP1345-079LF) connects the expanded C-patches to the main radiator. The status of the connection between the metals, which is controlled by the pin diodes, determines the effective resonant length of the antenna. This length is measured in wavelengths (open or short). Stubs in the L-shape are used to redistribute the surface currents. Because of the L-shaped inverted stubs placed into the top plane, the antenna can operate in a new pattern while maintaining a satisfactory gain and impedance matching.

Figure 4 illustrates the stages of development for the proposed antennas. A simple rectangular antenna fed by a 50 Ω microstrip line is depicted in Figure 4a. Figure 5 shows the evolution stages' coefficient of reflection characteristics. Poor impedance matching characterizes the rectangular antenna. In step 2, the radiator's edges are truncated, and in step 3, the C-shaped metal in the radiator's center is etched to minimize the antenna's physical size. To shift the concentration of surface currents, an L-shaped stub is inserted in step 4. This enables the antennas to work using a various pattern while preserving high gain and good impedance matching. The addition of resonant stubs causes slight changes in impedance matching that can be accounted for by loading a patch in the ground plane, as illustrated in Figure 1.

Figure 4. Evolution of the proposed system (a) step-1 (b) step-2 (c) step-3 and (d) step-4.

Figure 5. Reflection coefficients of the stage's development.
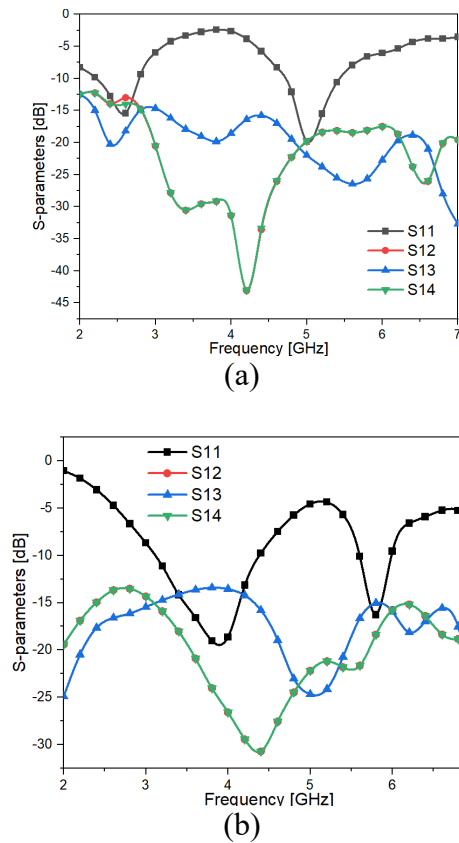
2.2 MIMO Antennas

To receive signals from all directions, automobile applications require many antennas. The proposed MIMO antennas are aligned orthogonally to one another to enhance isolation without using decoupling

mechanisms. Furthermore, the orthogonal arrangement provides polarization diversity.
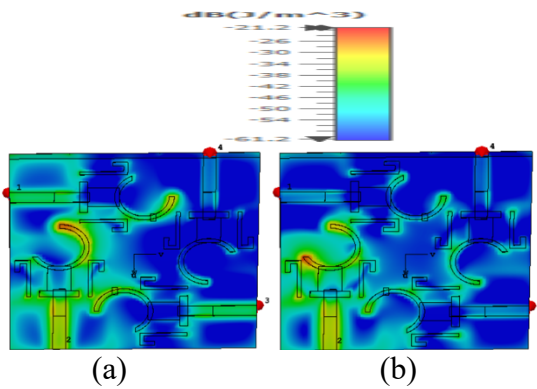
The inter-element spacing between the radiators is maintained at less than 1mm, and the dimensions of the MIMO antenna are 50 mm x 50 mm2. Figure 6 shows the MIMO diversity antenna's simulated S-parameters for the two states. According to specifications, the impedance bandwidth of these four element antennas ranges among four bands (2.29 - 2.75, 3.06 - 4.5, 4.658 - 5.49, 5.51 - 5.96 GHz). Figure 7 illustrates the mutual coupling between the radiators, which is quite strong. S12, S13, and S14 all have values larger than -13 dB, which can be seen in the plot of the surface current distribution at 2.5 and 5 GHz. Even if only the 1st antenna is active, the surface current will reach the other antenna components via the ground plane and enhance their connection. This is true even if the first antenna element is the only one that is activated. Previous publications had the ground planes of the antenna elements disconnected from one another. This causes a break in the surface current that flows between the antenna's elements. This improves their isolation and eliminates the need for separate decoupling networks.

The E-field plots of proposed MIMO antennas in three dimensions are depicted in Figure 8, and they are shown at a variety of resonant frequencies. On and off states of the proposed quad-port MIMO antenna are illustrated in Figure 9 as modelled radiation patterns in the XZ and YZ planes, respectively. When using simulated values, it can be seen that patterns are constant with regard to their orientation. Also, the amount of cross-polarization is at least as high as the amount of co-polarization. As a result, the proposed antenna's radiation properties are satisfactory.
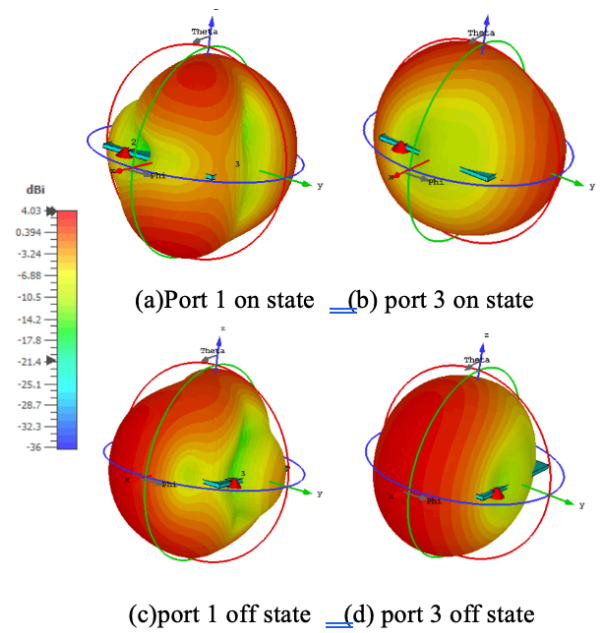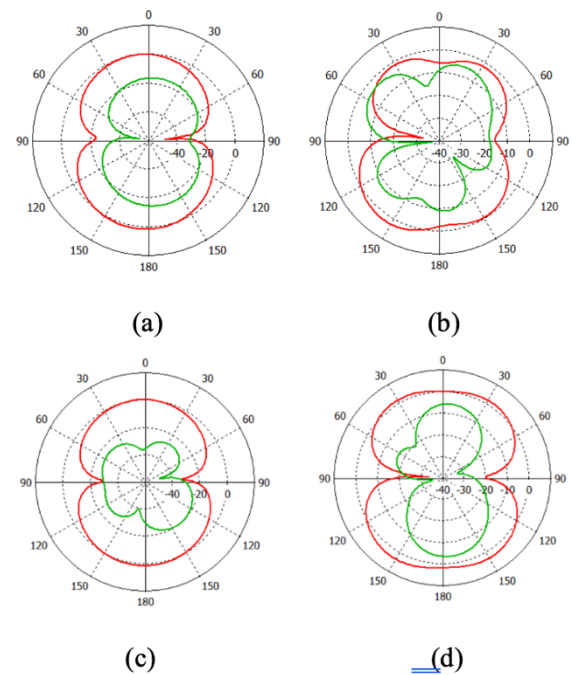
(a)

(b)

Figure 6. Reflection coefficient of the MIMO antennas (a) on state (b) off state.

(a)   (b)

Figure 7. Surface current distribution at (a) 2.5 and (b) 5 GHz.

(a)Port 1 on state   (b) port 3 on state

(c)port 1 off state   (d) port 3 off state

Figure 8. Three dimensional radiation pattern for two ports at two frequencies (a-b) at 5 GHz and (c-d) at 3.5 GHz.

(a)   (b)

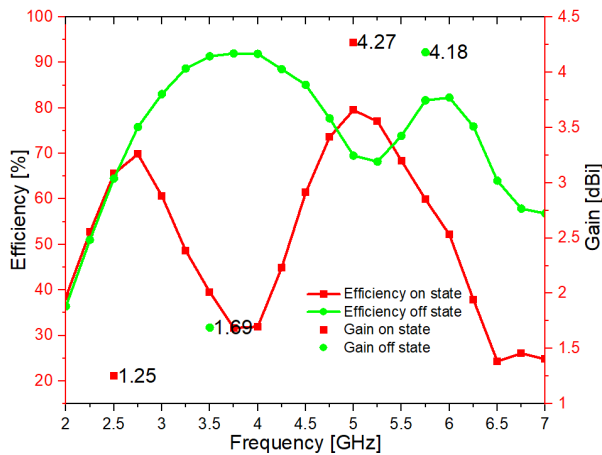(c)   (d)

Figure 9. Radiation pattern of E-field at XZ and YZ planes at (a) 2.5 GHz and (b) 5 GHz (c) 3.5 GHz and (d) 5.7 GHz.

With the remaining ports terminated with matching loads, it is possible to simulate Ant.1's two-dimensional (2D) XZ and YZ radiation patterns. Figure 9a and b show the radiation patterns for an ON diode at 2.5 GHz

and 5 GHz. Figures 9c and d show radiation patterns at 3.5 GHz and 5.7 GHz when the diode is off. At all of the given frequencies, the amplitude difference between the co-polarized and cross-polarized components was larger than 15 decibels at 90 degrees in both planes.

Figure 10 is a representation of the gain and efficiency graphs for the ON and OFF state of a PIN diode. The antenna operating bands range from 2.29 to 2.75 GHz; 3.06 to 4.5 GHz; 4.658 to 5.49 GHz; and 5.1 to 5.8 GHz. Within these frequency ranges, the minimum gain and efficiency are 1.25 dBi and 65%, respectively. However, the highest gain is 4.27 dBi, and the maximum efficiency is 94%. As can be observed in Figure 10, the drop in efficiency is mostly caused by the FR-4 substrate while it is in its off state. This is true for both the 3.06–4.5 GHz band as well as the 5.1–5.8 GHz band. Even though the efficiency has gone down, the final values in the working bands are still good with the design that was shown.

Figure 10. Gain and efficiency vs frequency for the on and off state.

3. Performance of the proposed MIMO antennas

The ECC and DG can be used to evaluate the diversity performance of a MIMO antenna. It is possible to determine the degree of spatial correlation or diversity between two antenna elements by performing an ECC calculation. For low-efficiency MIMO antennas, S-parameters can't be used to calculate ECC

[28]. So, for low-efficiency antennas, the ECC should be estimated from the radiation patterns in the far field. ECC may be evaluated for high-efficiency antennas by determining the correlation of losses [28]. A MIMO antenna with a radiation efficiency of greater than 50% is well-suited to this approach. The following equation can be used to obtain the guaranteed correlation coefficient in equation (3) and (4):

$$\left|\rho_{ij}\right|_{\text{guaranteed}} = \left|\rho_{ij}\right| + \sqrt{\left(\frac{1}{\eta_i}-1\right)\left(\frac{1}{\eta_i}-1\right)} \qquad \text{Eq.3}$$

Where

$$\rho_{ij} = \frac{-s_{ii}s_{ij}^* - s_{ji}s_{jj}^*}{\sqrt{\left(1-|s_{ii}|^2-|s_{ji}|^2\right)\left(1-|s_{jj}|^2-|s_{ij}|^2\right)\eta_i\eta_j}} \qquad \text{Eq.4}$$
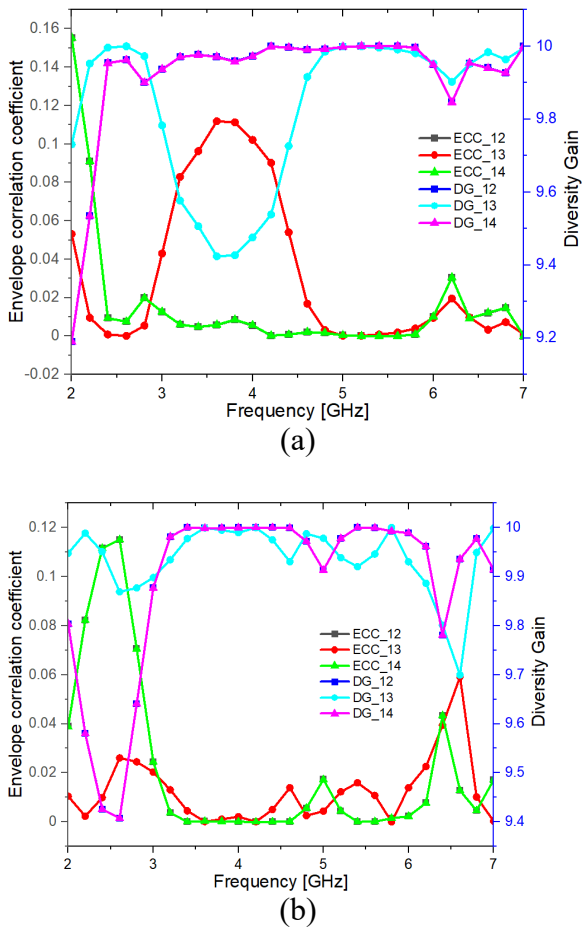
Where η_i and η_i refer to the 1st and 2nd antennas, respectively. After figuring out the correlation coefficient, we can solve the following equation to find the guaranteed value of ECC in equation (5):

$$\text{ECC}_{\text{guaranteed}} = \left|\rho_{ij}\right|^2 \text{ guaranteed} \qquad \text{Eq.5}$$

This method of determining ECC between the two antenna elements is used since the designed MIMO antennas demonstrates greater than 65% efficiency in the operational bands. A total of ECC between different antennas have been calculated and illustrated in Figures 11a and b. In addition, the ECC graphs for the ON and OFF state of the PIN diode are shown. MIMO antennas with ECC values below 0.16 in both working bands meet the commonly accepted standard (ECC < 0.5) for the MIMO antennas performance.

As for evaluating the MIMO performance, the DG is another essential factor to consider. The DG shows how the four elements outperform a single element in terms of performance. Ideal dynamic range (DG) is 10 decibels. The computed DG is 9.95 dB, as shown in Figures 11a and b for both states of the PIN diode using Equation (6) given below [28].

$$DG = 10\sqrt{\left(1-\left|0.99\rho_{ij}\right|^2\right)} \qquad \text{Eq.6}$$

Figure 11. Envelop correlation coefficient and diversity gain for to states (a) on state and (b) off state.

4. CONCLUSION

This paper presents compact reconfigurable quad-port MIMO antennas with orthogonal arrangements for sub-6 GHz band applications. PIN diode switches control the radiating antenna's parameters. The compound configuration uses PIN diodes as a switch to enable dual-band operations at 2.5 and 5 GHz in mode-1 (when the switch is on). At the same time, the antennas operate at 3.5 and 5.7 GHz in mode-2 using a different dual-band design (when the switch is OFF). The orthogonal arrangement of the antenna elements enhances inter-element isolation, resulting in a mutual coupling between MIMO antennas of less than 13 dB.
S-parameters, far-field radiation characteristics, surface current distribution, and MIMO performance metrics of the designed system are discussed and presented.

According to the data, the correlation is less than 0.16 dB, and the diversity gain is greater than 9.9 dB. Therefore, the proposed MIMO antenna could benefit wireless applications in the sub-6 GHz frequency range.

REFERENCES

[1]   S. Haykin, "Cognitive radio: Brain-empowered wireless communications," *IEEE Journal on Selected Areas in Communications*, vol. 23, no. 2, pp. 201–220, Feb. 2005.

[2]   J. Mitola, "Cognitive radio architecture evolution," *Proceedings of the IEEE*, vol. 97, no. 4, pp. 626–641, 2009.

[3]   F. Alsubaei, A. Abuhussein, and S. Shiva, "An Overview of Enabling Technologies for the Internet of Things," *Internet of Things A to Z*, pp. 77–112, May 2018.

[4]   K. Kanwal, G. A. Safdar, M. Ur-Rehman, and X. Yang, "Energy Management in LTE Networks," *IEEE Access*, vol. 5, pp. 4264–4284, 2017.

[5]   D. J. Lee, S. J. Lee, S. T. Khang, and J. W. Yu, "Extensible compact 8-port MIMO antenna with pattern gain," *Microwave and Optical Technology Letters*, vol. 59, no. 2, pp. 236–240, Feb. 2017.

[6]   J. Y. Deng, J. Yao, D. Q. Sun, and L. X. Guo, "Ten-element MIMO antenna for 5G terminals," *Microwave and Optical Technology Letters*, vol. 60, no. 12, pp. 3045–3049, Dec. 2018.

[7]   M. Abdullah, Q. Li, W. Xue, G. Peng, Y. He, and X. Chen, "Isolation enhancement of MIMO antennas using shorting pins," vol. 33, no. 10, pp. 1249–1263, Jul. 2019.

[8]   N. O. Parchin et al., "Mobile-phone antenna array with diamond-ring slot elements for 5G massive MIMO systems," Electronics (Switzerland), vol. 8, no. 5, May 2019.

[9]   G. J. Foschini and M. J. Gans, "On Limits of Wireless Communications in a Fading Environment when Using Multiple Antennas," Wireless Personal Communications 1998 6:3, vol. 6, no. 3, pp. 311–335, 1998.

[10] M. Johnny and M. R. Aref, "Blind interference alignment for the K-User SISO interference channel using reconfigurable antennas," IEEE Communications Letters, vol. 22, no. 5, pp. 1046–1049, May 2018.

[11] M. M. Hassan et al., "A novel UWB MIMO antenna array with band notch characteristics using parasitic decoupler," Journal of Electromagnetic Waves and Applications, vol. 34, no. 9, pp. 1225–1238, Jun. 2020.

[12] R. G. Vaughan and J. B. Andersen, "Antenna diversity in mobile communications," IEEE Transactions on Vehicular Technology, vol. 36, no. 4, pp. 149–172, 1987.

[13] R. Hussain, M. S. Sharawi, and A. Shamim, "4-Element concentric pentagonal slot-line-based ultra-wide tuning frequency reconfigurable MIMO antenna system," IEEE Transactions on Antennas and Propagation, vol. 66, no. 8, pp. 4282–4287, Aug. 2018.

[14] R. Hussain, A. Ghalib, and M. S. Sharawi, "Annular slot-based miniaturized frequency-agile MIMO antenna system," IEEE Antennas and Wireless Propagation Letters, vol. 16, pp. 2489–2492, Jul. 2017.

[15] R. Hussain, M. S. Sharawi, and A. Shamim, "An Integrated Four-Element Slot-Based MIMO and a UWB Sensing Antenna System for CR Platforms," IEEE Transactions on Antennas and Propagation, vol. 66, no. 2, pp. 978–983, Feb. 2018.

[16] J. H. Lim, Z. J. Jin, C. W. Song, and T. Y. Yun, "Simultaneous frequency and isolation reconfigurable MIMO PIFA using PIN diodes," IEEE Transactions on Antennas and Propagation, vol. 60, no. 12, pp. 5939–5946, 2012.

[17] Y. Li, C. Y. D. Sim, Y. Luo, and G. Yang, "Multiband 10-Antenna Array for Sub-6 GHz MIMO Applications in 5-G Smartphones," IEEE Access, vol. 6, pp. 28041–28053, May 2018.

[18] Y. Li, C. Y. D. Sim, Y. Luo, and G. Yang, "High-Isolation 3.5 GHz Eight-Antenna MIMO Array Using Balanced Open-Slot Antenna Element for 5G Smartphones," IEEE Transactions on Antennas and Propagation, vol. 67, no. 6, pp. 3820–3830, Jun. 2019.

[19] N. O. Parchin et al., "Eight-Element Dual-Polarized MIMO Slot Antenna System for 5G Smartphone Applications," IEEE Access, vol. 7, pp. 15612–15622, 2019.

[20] Y. Li, C. Y. D. Sim, Y. Luo, and G. Yang, "12-Port 5G Massive MIMO Antenna Array in Sub-6GHz Mobile Handset for LTE Bands 42/43/46 Applications," IEEE Access, vol. 6, pp. 344–354, Oct. 2017.

[21] Y. L. Ban, C. Li, C. Y. D. Sim, G. Wu, and K. L. Wong, "4G/5G Multiple Antennas for Future Multi-Mode Smartphone Applications," IEEE Access, vol. 4, pp. 2981–2988, 2016.

[22] G. Li, H. Zhai, Z. Ma, C. Liang, R. Yu, and S. Liu, "Isolation-improved dual-band MIMO antenna array for LTE/WiMAX mobile terminals," IEEE Antennas and Wireless Propagation Letters, vol. 13, pp. 1128–1131, 2014.

[23] Y. Liu, S. Wang, N. Li, J. B. Wang, and J. Zhao, "A compact dual-band dual-polarized antenna with filtering structures for sub-6 GHz base station applications," IEEE Antennas and Wireless Propagation Letters, vol. 17, no. 10, pp. 1764–1768, Oct. 2018.

[24] W. W. Lee and B. Jang, "A Tunable MIMO Antenna with Dual-Port Structure for Mobile Phones," IEEE Access, vol. 7, pp. 34113–34120, 2019.

[25] G. Jin, C. Deng, J. Yang, Y. Xu, and S. Liao, "A new differentially-fed frequency reconfigurable antenna for WLAN and sub-6GHz 5G applications," IEEE Access, vol. 7, pp. 56539–56546, 2019.

[26] Q. Chen et al., "Single ring slot-based antennas for metal-rimmed 4G/5G smartphones," IEEE Transactions on Antennas and Propagation, vol. 67, no. 3, pp. 1476–1487, Mar. 2019.

[27] S. Ullah, I. Ahmad, Y. Raheem, S. Ullah, T. Ahmad, and U. Habib, "Hexagonal shaped CPW Feed based Frequency Reconfigurable Antenna for WLAN and Sub-6 GHz 5G applications," 2020 International Conference on Emerging Trends in Smart Technologies, ICETST 2020, Mar. 2020.

[28]M. J. Farhan, and A. K. Jassim, "Design and Analysis a Frequency Reconfigurable Octagonal Ring-Shaped Quad-Port Dual-Band Antenna Based on a Varactor Diode," Progress In Electromagnetics Research C, vol. 116, pp. 235–248, 2021.